A Simulation Study on the Topotactic Transformations from Aluminophosphate $AlPO_4$-21 to $AlPO_4$-25

Jiyang Li, Jihong Yu, Kaixue Wang, Guangshan Zhu, and Ruren Xu*

State Key Laboratory of Inorganic Synthesis and Preparative Chemistry, Jilin University, Changchun 130023, P. R. China

Received March 16, 2001

Aluminophosphate $AlPO_4$-21 (AWO), formulated $|(CH_3)_2NH_2|[Al_3P_3O_{12}(OH)]$, has been synthesized solvothermally by using dimethylamine as the template. Single-crystal X-ray diffraction analysis shows that $AlPO_4$-21 crystallizes in the monoclinic space group $P2_1/n$ with $a = 8.687(2)$ Å, $b = 17.428(5)$ Å, $c = 9.159(2)$ Å, $\beta = 109.60(2)°$, $V = 1306.3(5)$ Å^3, and $Z = 4$. XRD analysis shows that $AlPO_4$-21 transforms to $AlPO_4$-25 (ATV) upon calcination at 500 °C. The molecular dynamics simulation approach was used to investigate the topotactic transformations from $AlPO_4$-21. The simulation study suggests that $AlPO_4$-21 is energetically favored to transform to $AlPO_4$-25, as well as other hypothetical forms, by the changing of the UUDD chains to the UDUD chains.

Introduction

A series of open-framework aluminophosphates (denoted $AlPO_4$-*n*) were first prepared by Wilson et al. in the early 1980s by using organic amines as the templates in a hydrothermal synthesis system.[1] Since then, there remains a considerable interest in developing new aluminophosphate materials with novel open-frameworks because of their widespread applications in catalysis, ion exchange, and gas separation, as well as in advanced materials and host−guest assembly chemistry. These materials typically possess three-dimensional (3D) neutral frameworks built up from the strict alternation of AlO_4 and PO_4 tetrahedra. In some cases, such as VPI-5, $AlPO_4$-12, -14, -15, -17, -21, and hydrates of AlPOs (including H1−H4),[2−11] five- or six-coordinated Al atoms exist which are coordinated to extra-framework H_2O molecules or OH groups. The extra-framework species and the occluded templates can be removed upon heating at high temperature, leaving an open-framework structure. Some topotactic transformations may occur during the calcination because the frameworks of these mixed-bonded compounds[12] deviate from the ideal (4,2)-connection found for typical zeolites. Notable examples are the transformations of the as-synthesized $AlPO_4$-21 to $AlPO_4$-25[13,14] and $AlPO_4$-C to $AlPO_4$-D[14,15] upon heating.

However, the nature of topotactic transformations is not yet well understood. Recently, computational simulation approaches played an important role in the study of the structures of open-framework materials.[16,17] For example, Gale et al. investigated the locations and diffusions of calcium cations in chabazite by computational methods.[18] Catlow et al. investigated the water adsorption in Heulandite-type zeolites by the Monte Carlo method.[19] Cox et al. determined the framework structure of ERS-7 by simulated annealing.[20] On the other hand, computer modeling approaches have greatly enhanced researchers' ability to elucidate the formation mechanism of microporous compounds, such as the nucleation, crystal growth, and templating effect in hydrothermal systems.[21] Lewis et al. described a method for the de novo design of template molecules that can be computationally "grown" in the desired inorganic framework.[22] Catlow et al. developed methodologies to determine the relative templating efficacy of an organic species within a large range of known zeolite frameworks.[23] We have recently investigated the templating effect in the formation of layered aluminophosphates in terms of nonbonding interactions between the host and the guest template.[24] In this work, we use dimethylamine as the template to synthesize $AlPO_4$-21, and its

(1) Wilson, S. T.; Lok, B. M.; Messina, C. A.; Cannan, T. R.; Flanigen, E. M. *J. Am. Chem. Soc.* **1982**, *104*, 1146.
(2) McCusker, L. B.; Baerlocher, C.; Jahn, E.; Bülow, M. *Zeolites* **1991**, *11*, 308.
(3) Parise, J. B. *J. Chem. Soc., Chem. Commun.* **1984**, 1449.
(4) Pluth, J. J.; Smith, J. V.; Bennett, J. M.; Cohen, J. P. *Acta Crystallogr.* **1984**, *C40*, 2008.
(5) Parise, J. B. *J. Chem. Soc., Chem. Commun.* **1985**, 606.
(6) Pluth, J. J.; Smith, J. V.; Bennett, J. M. *Acta Crystallogr.* **1986**, *C42*, 283.
(7) Bennett, J. M.; Cohen, J. M.; Artioli, G.; Pluth, J. J.; Smith, J. V. *Inorg. Chem.* **1985**, *24*, 188.
(8) Parise, J. B.; Day, C. S. *Acta Crystallogr.* **1985**, *C41*, 515.
(9) d'Yvoire, F. *Bull. Soc. Chim. Fr.* **1961**, 1762.
(10) Li, H.-X.; Davis, M. E. *J. Chem. Soc., Faraday Trans.* **1993**, *89*, 951.
(11) Pluth, J. J.; Smith, J. V. *Nature* **1985**, *318*, 165.
(12) Chen, J.; Pang, W.; Xu, R. *Top. Catal.* **1999**, 1.
(13) Richardson, J. W., Jr.; Smith, J. V.; Pluth, J. J. *J. Phys. Chem.* **1990**, *94*, 3365.
(14) Ryoo, M. H.; Chon, H. *J. Chem. Soc., Faraday Trans.* **1997**, *93*, 3259.
(15) Keller, E. B.; Meier, W. M.; Krichner, R. M. *Solid State Ionics* **1990**, *43*, 93.
(16) Catlow, C. R. A. *New Methods for Modeling Processes within Solids and at their Surfaces*; Oxford University Press: London, 1993.
(17) Catlow, C. R. A. *Computer Modeling in Inorganic Crystallography*; Academic Press: London, 1997.
(18) Grey, T.; Gale, J.; Nicholson, D.; Peterson, B. *Microporous Mesoporous Mater.* **1999**, *31*, 45.
(19) Channon, Y. M.; Catlow, C. R. A.; Jackson, R. A.; Owens, S. L. *Microporous Mesoporous Mater.* **1998**, *24*, 153.
(20) Campbell, B. J.; Bellussi, G.; Carluccio, L.; Perego, G.; Cheetham, A. K.; Cox, D. E.; Millini, R. *Chem. Commun.* **1998**, 1725.
(21) Catlow, C. R. A.; Coombes, D. S.; Lewis, D. W.; Pereira, J. C. G. *Chem. Mater.* **1998**, *10*, 3249.
(22) (a) Lewis, D. W.; Willock, D. J.; Catlow, C. R. A.; Thomas, J. M.; Hutchings, G. J. *Nature* **1996**, *382*, 604. (b) Lewis, D. W.; Sankar, G.; Wyles, J. K.; Thomas, J. M.; Catlow, C. R. A.; Willock, D. J. *Angew. Chem., Int. Ed. Engl.* **1997**, *36*, 2675.
(23) Lewis, D. W.; Freeman, C. M.; Catlow, C. R. A. *J. Phys. Chem.* **1995**, *99*, 11194.
(24) Li, J.; Yu, J.; Yan, W.; Xu, Y.; Xu, W.; Qiu, S.; Xu, R. *Chem. Mater.* **1999**, *11*, 2600.

10.1021/ic010292k CCC: $20.00
Published on Web 10/06/2001

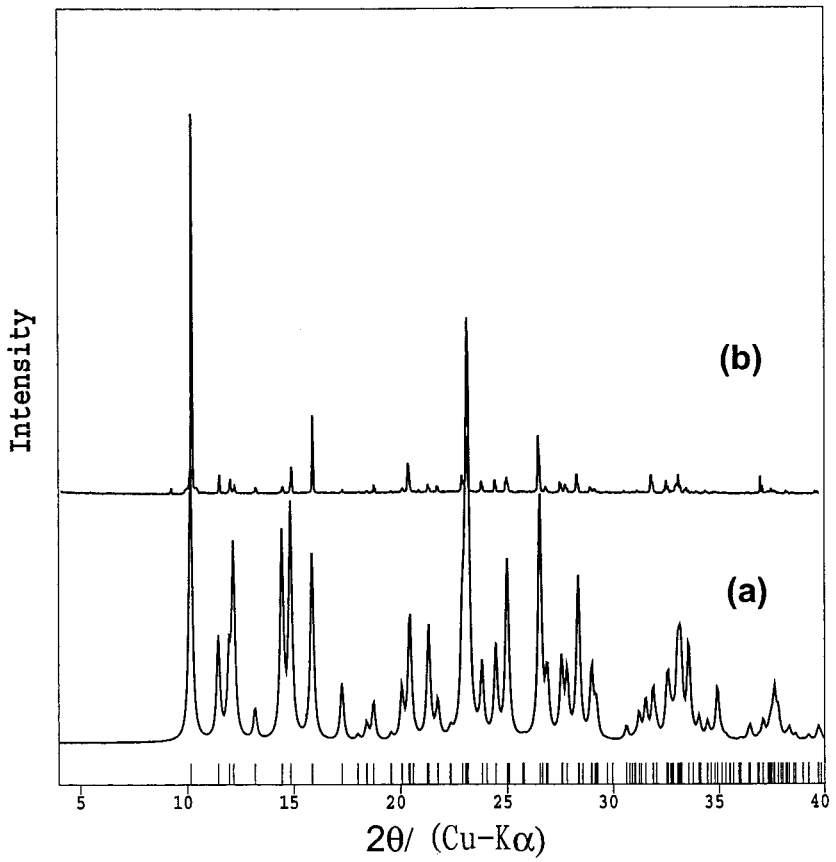

Figure 1. (a) Experimental X-ray powder diffraction pattern of $AlPO_4$-21 compared with (b) the simulated XRD pattern based on single-crystal structure analysis.

Table 1. Crystal Data and Structure Refinement for $|(CH_3)_2NH_2|[Al_3P_3O_{12}(OH)]$

fw	428.95
temp	293(2) K
wavelength	0.71073 Å
space group	monoclinic, *P*2(1)/*n*
a (Å)	8.6868(19)
b (Å)	17.428(5)
c (Å)	9.1589(17)
β (deg)	109.604(17)
V (Å^3)	1306.3(5)
Z	4
ρ_{calcd} (Mg m^{-3})	2.181
μ (mm^{-1})	0.731
final *R* indices [$I > 2\sigma(I)$][a]	$R_1 = 0.0380$, w$R_2 = 0.0806$
R indices (all data)	$R_1 = 0.0693$, w$R_2 = 0.0903$

[a] $R_1 = \Sigma(\Delta F/\Sigma(F_o))$; w$R_2 = (\Sigma[w(F_o^2 - F_c^2)])/\ \Sigma[w(F_o^2)^2]^{1/2}$, $w = 1/\sigma^2(F_o^2)$.

topotactic transformations are investigated using the molecular dynamics simulation approach. This highlights the possibility of using computational approaches to explore the thermodynamics stabilities of as-synthesized open-framework structures.

Experimental Section

Synthesis. The synthesis of $AlPO_4$-21 was carried out in a predominantly nonaqueous system in which ethylene glycol (EG) was used as the solvent, and dimethylamine was used as the template. The typical synthesis procedure was as follows: aluminum triisopropoxide [Al(^{i}PrO)$_3$] was first dispersed in ethylene glycol with stirring, phosphoric acid (H_3PO_4 85%, in water) was then added dropwise, and the reaction mixture was stirred until it was homogenenous. Finally, dimethylamine was added slowly to the above reaction mixture, and a gel with a molar composition of 1.0 Al(^{i}PrO)$_3$:1.8 H_3PO_4:1.5 dimethylamine:35.9 EG:1.7 H_2O was formed. The gel was stirred about 2 h at room temperature, sealed into a Teflon-lined stainless steel autoclave, and heated under static conditions for 20 d at 180 °C. The resulting product containing large single crystals of $AlPO_4$-21 was collected by filtration, washed with distilled water, and dried in air at 60 °C overnight. The $AlPO_4$-25 sample was obtained by calcining $AlPO_4$-21 at 500 °C for 5 h in air.

Characterization. The X-ray powder diffraction (XRD) patterns were recorded on a Siemens D5005 diffractometer with CuKα radiation (λ = 1.5418 Å). Thermogravimetric (TG) and differential thermal analysis (DTA) were performed on a Perkin-Elmer TGA-7 thermogravimetric analyzer and on a DTA-1700 differential thermal analyzer, respectively, in air atmosphere at a heating rate of 10 K min^{-1}.

Single-Crystal Structural Analysis. A suitable single crystal with size dimensions 0.08 × 0.08 × 0.06 mm was selected for X-ray diffraction analysis. The intensity data were collected on a Siemens SMART diffractometer equipped with a CCD bidimensional detector using graphite-monochromatic MoKα radiation (λ = 0.71073 Å) at a temperature of 20 ± 2 °C. Data processing was accomplished with the SAINT processing program.[25] The crystal structure was solved by direct methods with the SHELXTL software package,[26] and the heaviest atoms (Al and P) were easily located. Framework oxygen atoms were subsequently located in the difference Fourier maps, and the hydrogen atoms of the dimethylamine molecule were placed geometrically. All non-hydrogen atoms were refined anistropically. Crystal data and details of the data collection are given in Table 1.

Simulation Method. Computational simulations were carried out using the classical molecular dynamics (MD) simulation method[27] in the Cerius^2 package.[28] Several simulation models were designed from the initial experimental structure of $AlPO_4$-21 ($|NC_2H_8|[Al_3P_3O_{12}(OH)]$). First, the bridging hydroxyl groups bonded to the Al atoms and the

(25) SMART and SAINT (software package), Siemens Analytical X-ray Instruments Inc., Madison, WI, 1996.
(26) SHELXTL version 5.1, Siemens Industrial Automation Inc., 1997.
(27) Jackson, R. A.; Catlow, C. R. A. *Mol. Simul.* **1988**, *1*, 207.
(28) Cerius2, Molecular simulations/Biosym Corp., 1995.

Table 2. Atomic Coordinates ($\times 10^4$) and Equivalent Isotropic Displacement Parameters U(eq) ($Å^2 \times 10^3$) for $|(CH_3)_2NH_2|[Al_3P_3O_{12}(OH)]$

atom	x	y	z	U(eq)[a]	atom	x	y	z	U(eq)[a]
P(2)	7963(2)	2117(1)	9728(2)	15(1)	O(2)	4468(4)	889(2)	7680(4)	20(1)
P(1)	3402(2)	704(1)	8682(2)	14(1)	O(12)	12333(4)	3907(2)	8698(4)	18(1)
P(3)	12479(2)	3377(1)	10051(2)	15(1)	O(11)	12267(4)	2538(2)	9553(4)	18(1)
Al(1)	5097(2)	1689(1)	6897(2)	16(1)	O(10)	10420(4)	2901(2)	6788(5)	18(1)
Al(2)	6383(2)	1113(1)	11638(2)	13(1)	O(9)	9149(4)	1510(2)	6278(4)	18(1)
Al(3)	10647(2)	2040(1)	7973(2)	15(1)	O(5)	7741(4)	1438(2)	10681(4)	19(1)
O(1)	2806(4)	−118(2)	8400(4)	16(1)	O(3)	4406(4)	832(2)	10376(4)	16(1)
O(4)	6353(4)	2267(2)	8379(4)	21(1)	O(13)	11173(4)	3628(2)	10732(4)	24(1)
O(6)	8357(4)	2836(2)	10745(4)	19(1)	C(1)	1294(9)	641(4)	4091(9)	59(2)
O(7)	9329(4)	1945(2)	9107(4)	21(1)	N(1)	709(6)	111(3)	2774(6)	32(1)
O(8)	11901(4)	1211(2)	8195(4)	19(1)	C(2)	1696(10)	155(5)	1743(9)	66(2)

[a] U(eq) is defined as one-third of the trace of the orthogonalized U_{ij} tensor.

Table 3. Selected Bond Lengths (Å) and Bond Angles (deg) for $|(CH_3)_2NH_2|[Al_3P_3O_{12}(OH)]$[a]

P(2)−O(7)	1.508(4)	Al(1)−O(4)	1.748(4)
P(2)−O(5)	1.520(4)	Al(2)−O(5)	1.783(4)
P(2)−O(6)	1.531(4)	Al(2)−O(3)	1.787(4)
P(2)−O(4)	1.546(4)	Al(2)−O(12)#4	1.788(4)
P(1)−O(8)#1	1.513(4)	Al(2)−O(1)#5	1.877(4)
P(1)−O(1)	1.516(4)	Al(2)−O(10)#4	1.936(4)
P(1)−O(3)	1.520(4)	Al(3)−O(8)	1.780(4)
P(1)−O(2)	1.541(4)	Al(3)−O(7)	1.793(4)
P(3)−O(12)	1.517(4)	Al(3)−O(10)	1.823(4)
P(3)−O(9)#2	1.521(3)	Al(3)−O(11)	1.861(4)
P(3)−O(11)	1.525(4)	Al(3)−O(9)	1.898(4)
P(3)−O(13)	1.531(4)	O(10)−H(3)	0.87(2)
Al(1)−O(13)#3	1.728(4)	C(1)−N(1)	1.468(8)
Al(1)−O(6)#3	1.736(4)	N(1)−C(2)	1.475(8)
Al(1)−O(2)	1.737(4)		
O(7)−P(2)−O(5)	109.2(2)	O(5)−Al(2)−O(3)	114.81(18)
O(7)−P(2)−O(6)	110.4(2)	O(5)−Al(2)−O(12)#4	112.23(18)
O(5)−P(2)−O(6)	109.5(2)	O(3)−Al(2)−O(12)#4	132.88(19)
O(7)−P(2)−O(4)	110.3(2)	O(5)−Al(2)−O(1)#5	88.24(17)
O(5)−P(2)−O(4)	109.6(2)	O(3)−Al(2)−O(1)#5	91.13(16)
O(6)−P(2)−O(4)	107.8(2)	O(12)#4−Al(2)−O(1)#5	87.60(17)
O(8)#1−P(1)−O(1)	106.9(2)	O(5)−Al(2)−O(10)#4	97.22(18)
O(8)#1−P(1)−O(3)	111.0(2)	O(3)−Al(2)−O(10)#4	86.86(16)
O(1)−P(1)−O(3)	111.0(2)	O(12)#4−Al(2)−O(10)#4	90.04(18)
O(8)#1−P(1)−O(2)	109.4(2)	O(1)#5−Al(2)−O(10)#4	174.52(17)
O(1)−P(1)−O(2)	109.6(2)	O(8)−Al(3)−O(7)	110.12(18)
O(3)−P(1)−O(2)	108.9(2)	O(8)−Al(3)−O(10)	132.50(19)
O(12)−P(3)−O(9)#2	108.8(2)	O(7)−Al(3)−O(10)	117.31(18)
O(12)−P(3)−O(11)	111.8(2)	O(8)−Al(3)−O(11)	90.86(17)
O(9)#2−P(3)−O(11)	109.6(2)	O(7)−Al(3)−O(11)	93.18(17)
O(12)−P(3)−O(13)	106.7(2)	O(10)−Al(3)−O(11)	88.99(18)
O(9)#2−P(3)−O(13)	108.4(2)	O(8)−Al(3)−O(9)	85.59(17)
O(11)−P(3)−O(13)	111.4(2)	O(7)−Al(3)−O(9)	91.91(17)
O(13)#3−Al(1)−O(6)#3	108.54(19)	O(10)−Al(3)−O(9)	90.37(18)
O(13)#3−Al(1)−O(2)	107.99(19)	O(11)−Al(3)−O(9)	174.56(18)
O(6)#3−Al(1)−O(2)	107.65(18)	Al(3)−O(10)−Al(2)#7	144.0(2)
O(13)#3−Al(1)−O(4)	109.73(19)	Al(3)−O(10)−H(3)	110(4)
O(6)#3−Al(1)−O(4)	112.72(19)	Al(2)#7−O(10)−H(3)	106(4)
O(2)−Al(1)−O(4)	110.08(19)	C(1)−N(1)−C(2)	112.2(6)

[a] Symmetry transformations used to generate equivalent atoms: #1 $x-1, y, z$; #2 $x+1/2, -y+1/2, z+1/2$; #3 $x-1/2, -y+1/2, z-1/2$; #4 $x-1/2, -y+1/2, z+1/2$; #5 $-x+1, -y, -z+2$; #6 $x+1, y, z$; #7 $x+1/2, -y+1/2, z-1/2$.

occluded templates were removed from $AlPO_4$-21 leaving a neutral open-framework structure with an empirical formula of $Al_{12}P_{12}O_{48}$, denoted **Model1**. Then, the crystal symmetry of **Model1** was decreased to $P1$. Next, starting from **Model1**, several hypothetical structures (denoted **H**−***n***) were designed by changing the connections between the Al and P atoms among the three-connected 2D (4.6.8), (6.8.8) nets in **Model1**. Finally, the energy-minimization and the molecular dynamics simulation approaches were used to optimize the structures of the designed models. The Burchart 1.01 force field,[29] which is used to treat the frameworks of zeolites, was chosen. In this paper, we mainly study the energies (E_f) of inorganic frameworks that include bonds and Urey−Bradley, van der Waals (VDW), and electrostatic energies.

(29) de Vos Burchart, E. Studies on Zeolites; Molecular Mechanics, Framework Stability, and Crystal Growth. Ph.D. Thesis, Technische Universiteit Delft, 1992.

Results and Discussion

The X-ray diffraction (XRD) pattern of the as-synthesized $AlPO_4$-21 is shown in Figure 1, which is in good agreement with the simulated XRD pattern based on single-crystal structure analysis. This proves that the as-synthesized product is a single phase. Single-crystal analysis shows that $AlPO_4$-21 crystallizes in the monoclinic space group $P2_1/n$ with $a = 8.687(2)$ Å, $b = 17.428(5)$ Å, $c = 9.159(2)$ Å, and $\beta = 109.60(2)°$. The atomic coordinates, and the selected bond distances and angles for $AlPO_4$-21 are presented in Tables 2 and 3, respectively.

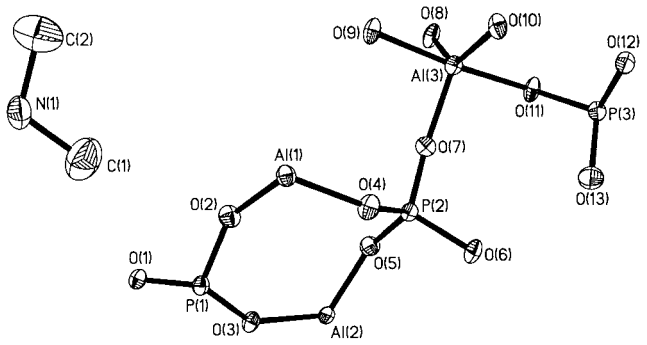

Figure 2. Thermal ellipsoid plot (50% probability) of a section of the structure of $AlPO_4$-21 showing the atom labeling, the coordination about the independent Al and P atoms, and the template.

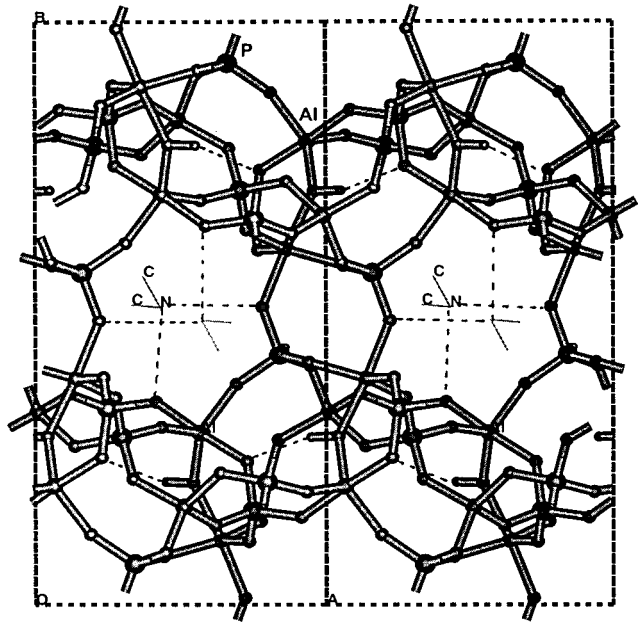

Figure 3. Open-framework structure of $AlPO_4$-21 along the [001] direction.

Figure 2 shows one asymmetric unit which contains three crystallographically distinct Al sites and three crystallographically distinct P sites. Each P atom shares four oxygens with adjacent Al atoms. The P−O bond lengths (1.508(4)−1.546(4) Å) and O−P−O bond angles (106.7(2)−111.8(2)°) are typical for aluminophosphate compounds. Of the three crystallographically distinct Al sites, Al(1) is in the near-regular tetrahedral environment. The Al(1)−O(2) and Al(1)−O(4) bond lengths are 1.737(4) and 1.748(4) Å, respectively. The O(2)−Al(1)−O(4) bond angle is 110.1(2)°. The other two Al sites, Al(2) and Al(3), are five-coordinated with a shared bridging hydroxyl group. Each Al also shares four bridging oxygens with phosphorus atoms. The Al(2)−O and Al(3)−O bond lengths range between 1.780(4) and 1.898(4) Å, and the O−Al(2)−O and O−Al(3)−O bond angles vary from 85.6(17) to 174.6(2)° which deviate from those of regular AlO_4 tetrahedra. The alternation of Al units (including AlO_4 and AlO_5) and PO_4 tetrahedra constructs a three-dimensional framework. Figure 3 shows the open-framework structure of $AlPO_4$-21 viewed along the [001] direction. It consists of eight-membered ring (MR) channels surrounded by four AlO_5 units and four PO_4 units. There are H-bonds between the framework oxygen O(11) and the hydroxyl group in the 5-MR. Two protonated dimethylamine molecules, $(CH_3)_2NH_2^+$, locate in the 8-MR channels and interact with the framework oxygens through H-bonds. The distances of N(1)···O(1) and N(1)···O(9) are 2.877 and 2.945 Å, respectively.

The TG−DTA curves of $AlPO_4$-21 are given in Figure 4. An obvious weight loss of ca. 15.0 wt % in the region of 340−450 °C (calcd 14.7 wt %) occurs. A strong endothermic peak from the decomposition of the organic templates is observed at ca. 390 °C, while a weak exothermic peak is observed at ca. 440 °C due to the desorption of the OH groups. XRD study shows that the structure of $AlPO_4$-21 converts to $AlPO_4$-25 with the loss of the OH groups between the Al atoms and the encapsulated organic species upon heating at 500 °C (Figure 5). It was originally speculated that the structure of $AlPO_4$-25 contains the same type of three-connected 2D nets as $AlPO_4$-21. It was later determined that it has up−down−up−down (UDUD) narsarsukite-type chains (Figure 6a) instead of the up−up−down−down (UUDD) double-crankshaft chains (Figure 6b) of $AlPO_4$-21.

We use the molecular dynamics simulation approach to study the topotactic transformation from $AlPO_4$-21 to $AlPO_4$-25. Several simulation models have been designed from the structure of $AlPO_4$-21 as mentioned in the Experimental Section. In **Model1,** all three inequivalent Al atoms and three inequivalent P atoms are in tetrahedral coordination, and the neutral framework has a formula of $Al_{12}P_{12}O_{48}$. However, two types

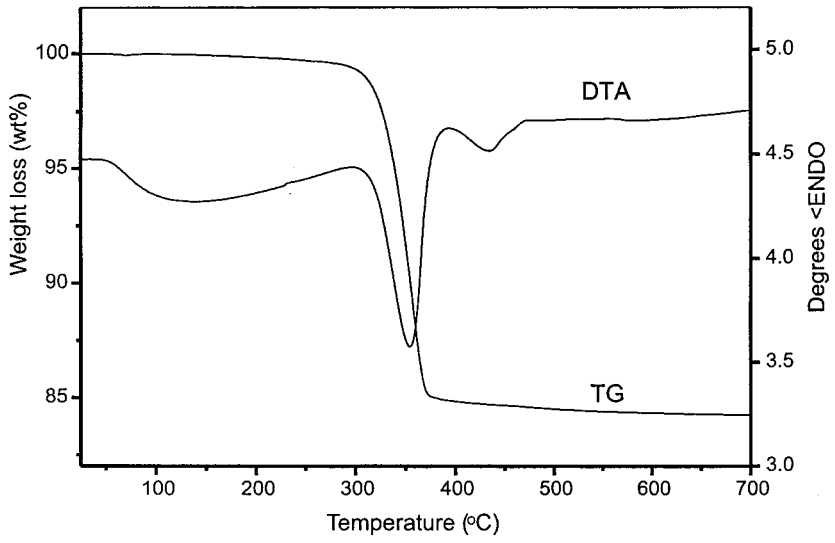

Figure 4. DTA and TG profiles of $AlPO_4$-21.

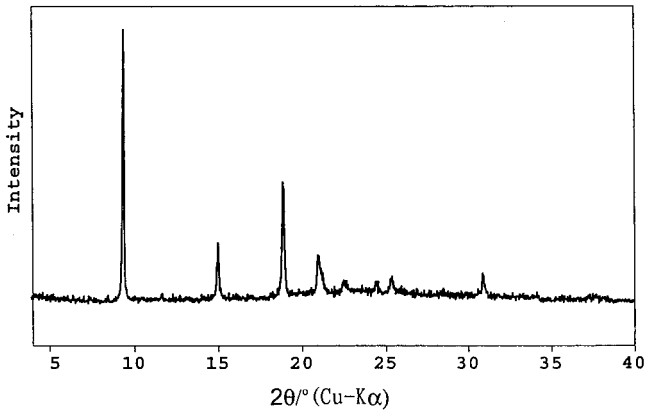

Figure 5. XRD pattern for $AlPO_4$-25 obtained after calcination of $AlPO_4$-21 at 500 °C.

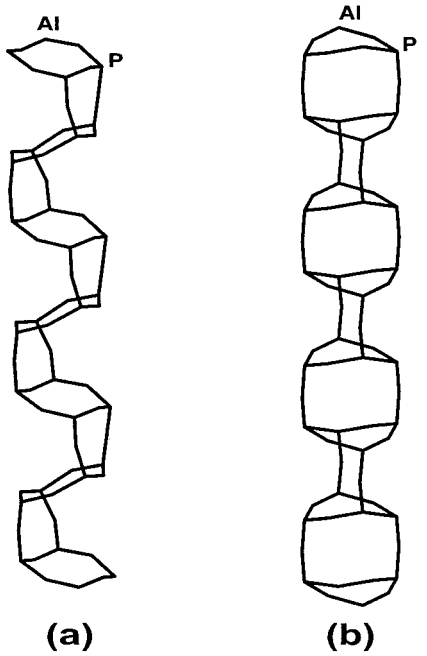

Figure 6. (a) The up−up−down−down double-crankshaft chain and (b) the up−down−up−down narsarsukite-type chain.

of Al atoms that emanate from the original five-coordinated Al atoms are in highly distorted tetrahedral environments. The Al−O−Al bond angles range from 85.6° to 174.6°. The framework energy (E_f) of **Model1** is −1615.61 kJ/mol per T atom which is higher than those of typical aluminophosphates such as −1655.74, −1661.30, and −1649.01 kJ/mol for $AlPO_4$-5, -8, and -11 per T site, respectively. This is due to its higher Urey−Bradley energy in **Model1**. During energy optimization, the structure of **Model1** converts rapidly toward the structure where all of the Al atoms are in regular tetrahedral environments (O−Al−O bond angles: 107.4°−111.2°) with a final E_f energy of −1664.31 kJ/mol per T atom. The optimized structure of **Model1** is in the monoclinic space group $P2_1/c$, the same as that of $AlPO_4$-21.

Starting from **Model1**, one hypothetical model (**H-1**) with a structure analogous to $AlPO_4$-25 is designed by changing the UUDD chains in **Model1** to the UDUD chains as in $AlPO_4$-25. The 3D framework structure of **H-1** is built up by the strict alternation of UDUD connections between 2D nets. It contains an eight-membered ring channel surrounded by four and six rings along the [001] direction. After structure optimization, the open-framework structure of **H-1** (Figure 7a) is in agreement

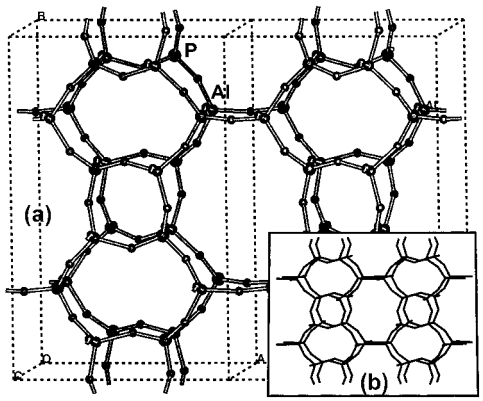

Figure 7. (a) Structure of predicted **H-1** from $AlPO_4$-21 and inserted (b) reported structure of $AlPO_4$-25.

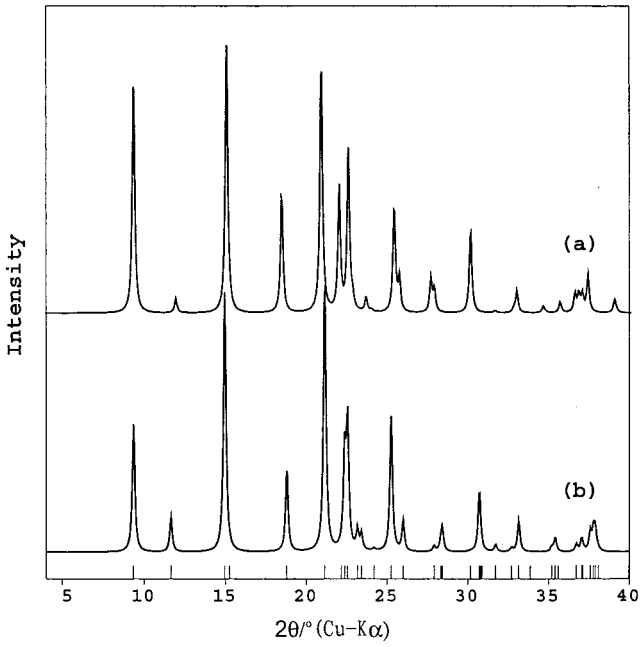

Figure 8. (a) The simulated XRD patterns for predicted **H-1** and (b) reported $AlPO_4$-25.

with the calcined structure of $AlPO_4$-21, namely $AlPO_4$-25 (Figure 7b). The simulated XRD pattern of **H-1** (Figure 8a) is consistent with that reported for $AlPO_4$-25[13] (Figure 8b). In the optimized structure of **H-1**, the calculated Al−O bond lengths and O−Al−O bond angles range from 1.724 to 1.734 Å and from 107.8° to 110.8°, respectively, which are typical for aluminophosphates as noted above. In addition, the calculated crystal system of **H-1** listed in Table 4 is similar to that of $AlPO_4$-25. The crystal symmetry of **H-1**, orthorhombic space group *Abm2*, is the same as that reported for $AlPO_4$-25[13] if we distinguish the Al and the P atoms instead of the T atoms.

As we noted, the topotactic transformation from $AlPO_4$-21 to $AlPO_4$-25 is due to the change of the UUDD chains to the UDUD chains. So, we investigate the energies of these two chains. The energies in their free forms are very similar, that is, −2200.57 and −2200.39 kJ/mol per T site, respectively. This indicates that these two chains easily transform to each other at high temperature. This is consistent with the experimental result that the as-synthesized $AlPO_4$-21 containing the UUDD chains can convert to $AlPO_4$-25 containing the UUDD chains upon calcination at 500 °C. Based on this, five hypothetical 3D frameworks (denoted **H**−***n***, $n = 2-6$) with the formula of $Al_{12}P_{12}O_{48}$ are designed as seen in Figure 9. They all have the

Table 4. The Calculated Results for the Predicted Structures Transformed from $AlPO_4$-21 Compared with Those of the Experimental and Optimized Structure of $AlPO_4$-25

name	space group	cell parameters (Å)	E_f (kJ/mol per T site)
H-1	*Abm2*	$a = 9.710$, $b = 15.126$, $c = 8.570$	−1664.73
H-2	*Cmca*	$a = 15.577$, $b = 8.675$, $c = 19.363$	−1662.47
H-3	*Cmca*	$a = 15.291$, $b = 8.721$, $c = 18.639$	−1663.22
H-4	*Abm2*	$a = 9.617$, $b = 5.445$, $c = 8.917$	−1662.51
H-5	*Pmna*	$a = 5.542$, $b = 8.346$, $c = 18.917$	−1653.77
H-6	*Cm*	$a = 9.614$, $b = 15.436$, $c = 9.687$, $\beta = 89.17$	−1650.55
$AlPO_4$-25(exp.)	*Acmm*	$a = 9.449$, $b = 15.203$, $c = 8.408$	−1660.88
$AlPO_4$-25(opt.)		$a = 9.710$, $b = 15.126$, $c = 8.570$	−1664.73

same type of three-connected 2D nets and the UDUD narsarsukite-type chains as **H-1**, but the connections between the 2D nets are different. In **H-2**, the connections around each 4-MR, 6-MR, and 8-MR are the UDUD, UUUDDD, and UUUUDDDD sequences, respectively. **H-3** is characterized by a UDUD, UDUDUD, and UUDUDDUD sequence around each 4-, 6-, and 8-MR. The connections between 2D nets parallel to the *ab* plane in **H-4** are similar with those of **H-2**, but the connection sequence around the 8-MR is UUDDUUDD in **H-4** and UUUUDDDD in **H-2**. The structures of **H-5** and **H-6** are different from other designed models; they both have UUUDUD-connected 6-MR, and their connection sequences around the 8-MR are UUDUUUUD and UUUDUUUD, respectively. The calculated crystal systems of **H-2**, **H-3, H-4, H-5**, and **H-6** are listed in Table 4 compared with those of **H-1** and the experimental and optimized structures of $AlPO_4$-25.[13] Interestingly, energy calculation results show that the structure of **H-1** is the most energetically favorable transformation formed from $AlPO_4$-21. It has the lowest E_f value, −1664.73 kJ/mol per T site, in our designed models. It is the same as the optimized structure of $AlPO_4$-25. This is agreeable with the experimental phenomenon. The E_f values of the predicted structures **H-2**, **H-3**, and **H-4** ranging from −1662.47 to −1663.22 kJ/mol per T site are similar to those of typical aluminophosphates such as −1663.11, −1662.62, and −1664.60 kJ/mol per T site for the optimized $AlPO_4$-5, -8, and -11, respectively. This means that they might be obtained under certain conditions. However, the E_f values of **H-5** and **H-6** are −1653.77 and −1650.55 kJ/mol per T site, respectively, which are higher than those of **H-2**, **H-3,** and **H-4,** as well as the typical aluminophosphates.

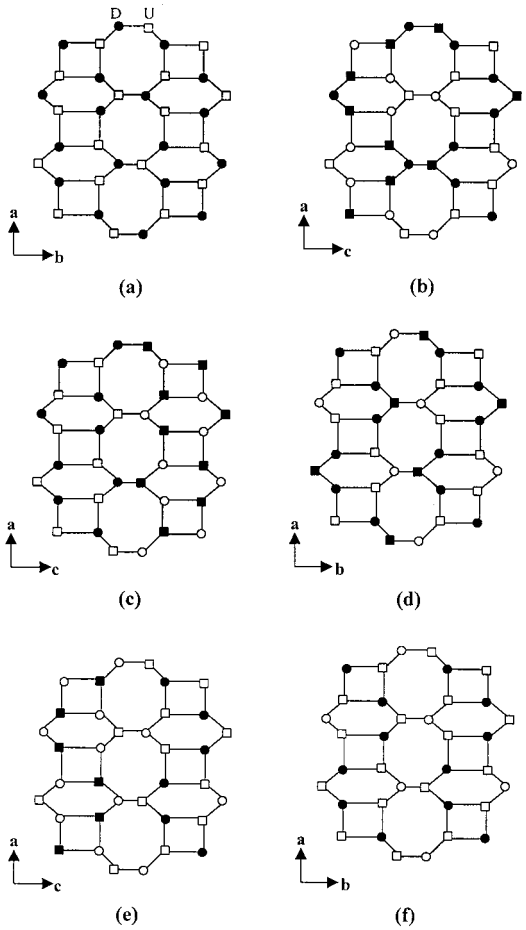

Figure 9. Projections of the connectivities of 2D nets in hypothetical structures for calcined $AlPO_4$-21 (a) **H-1**, (b) **H-2**, (c) **H-3**, (d) **H-4**, (e) **H-5**, and (f) **H-6**. Open symbol is up (U) and closed symbol is down (D); circular and square symbols represent the Al and P atoms, respectively.

Conclusion

$AlPO_4$-21 is prepared by using dimethylamine as the template, and its crystal structure has been described. It converts to $AlPO_4$-25 with the loss of OH groups and the encapsulated organic species after heating at 500 °C for 5 h. The topotactic transformation from $AlPO_4$-21 to $AlPO_4$-25 has been investigated using computational simulation approaches. Starting from the as-synthesized $AlPO_4$-21, the hypothetical model with a structure analogous to $AlPO_4$-25, as well as several new hypothetical 3D frameworks, has been designed by changing the UUDD chains to the UDUD chains. The simulation results show that $AlPO_4$-21 is energetically favorable and is likely to transform to $AlPO_4$-25. The structure of **H-1** is agreeable with the structure of $AlPO_4$-25 as reported before. Furthermore, some hypothetical structures are also energetically stable which might exist under certain conditions. This work will further assist in the rational design and synthesis of new 3D frameworks with specific structures.

Acknowledgment. We are grateful to the State Basic Research Project (G2000077507) and the National Natural Science Foundation of China for financial support. J.Y. is thankful for the support by TRAPOYT of MOE, P.R.C.

Supporting Information Available: One X-ray crystallographic file in CIF format. This material is available free of charge via the Internet at http://pubs.acs.org.

IC010292K